

Article

Mathematics Applications to Detect Fetal Syndromes

Faten Hameed Sabty*¹

1. Scientific Research Commission, Baghdad, Iraq

* Correspondence: hameedfaten6@gmail.com

Abstract: This research addresses the detection of fetal syndromes as a high-dimensional, non-linear binary classification problem, we mathematically formulate and empirically evaluate three classes of models: probabilistic classifiers based on Bayesian inference with multivariate Gaussian assumptions, geometric classifiers such as Support Vector Machines with non-linear kernels, and deep learning models based on multi-layer neural networks, the study's central hypothesis posits that the complex, synergistic interplay between sonographic and biochemical markers can only be captured by models with high representational capacity. Using a large clinical dataset, we demonstrate the hierarchical superiority of a Deep Neural Network (DNN), which achieved a test set Area Under the Curve (AUC) of 0.982 and a Matthews Correlation Coefficient (MCC) of 0.869, through the application of SHapley Additive exPlanations (SHAP), we deconstruct the model to reveal that higher-order interaction effects account for approximately 20% of its predictive power. Furthermore, by employing a Bayesian Neural Network (BNN), we introduce a framework for quantifying predictive uncertainty, decomposing it into its aleatoric and epistemic components, the results show that the BNN can reliably flag atypical patient profiles by exhibiting high epistemic uncertainty, a critical feature for clinical safety, this work concludes that the problem's underlying geometry is that of complex, intertwined manifolds, and that models capable of learning these structures while quantifying their own uncertainty represent the next frontier in prenatal diagnostics.

Keywords: Fetal Syndromes, Monogenic Disorders, Mathematical Modeling, Deep Learning, Bayesian Neural Networks, Uncertainty Quantification, Non-Linear Classification

Citation: Sabty, F. H. Mathematics Applications to Detect Fetal Syndromes. Central Asian Journal of Mathematical Theory and Computer Sciences 2025, 6(4), 992-1006.

Received: 10th Aug 2025

Revised: 20th Aug 2025

Accepted: 16th Sep 2025

Published: 24th Sep 2025



Copyright: © 2025 by the authors. Submitted for open access publication under the terms and conditions of the Creative Commons Attribution (CC BY) license (<https://creativecommons.org/licenses/by/4.0/>)

1. Introduction

The detection of fetal syndromes, stemming from monogenic disorders with severe systemic consequences such as premature cardiovascular diseases that alter an individual's life trajectory [1], necessitates its abstraction from a purely clinical context into a rigorous mathematical formulation, we can formally define this challenge as a binary classification problem: given a feature vector x belonging to the real Euclidean space \mathbb{R}^n , which embodies a series of biomedical measurements, and a binary response variable $y \in \{0, 1\}$ indicating the presence or absence of a syndrome, the fundamental challenge lies in constructing a classification function $f: \mathbb{R}^n \rightarrow \{0, 1\}$ that minimizes the expected classification error, this transition from diagnosis based on expertise to objective quantitative models is not merely a procedural enhancement but a philosophical shift that permits the rigorous mathematical validation and evaluation of models. At the heart of this challenge lies the task of decoding complex sequential data, where models like Long Short-Term Memory (LSTM) networks combined with ensemble learning have proven

their ability to extract precise information from protein sequences [2], a methodology adaptable to the analysis of genomic sequences, to maximize accuracy, more complex mathematical structures such as stacked ensemble classifiers are employed, along with advanced feature optimization techniques like recursive feature elimination, which allow for the identification of the most disease-relevant genomic patterns from a vast sea of noisy data [3].

The significance of these mathematical models becomes evident when considering specific diseases like sickle cell anemia, a devastating monogenic disorder that requires absolute diagnostic precision to enable advanced therapeutic interventions such as gene therapy [4]. Our deep understanding of the complex pathophysiology of such diseases [5] confirms that the relationships between genotype and phenotype are neither simple nor linear, with the advent of non-invasive prenatal diagnosis (NIPD) technologies, which rely on the analysis of cell-free DNA (cfDNA) using molecular "barcode" systems to identify disorders like β -thalassemia [6], we are faced with a deluge of high-dimensional data that necessarily demands sophisticated mathematical algorithms for its decoding, this escalating complexity has driven the development of deep neural networks, yet their predictive power has come at the cost of transparency, giving rise to a vital new field focused on developing explainable deep neural networks that not only provide a prediction but also mathematically justify their decision, an indispensable feature in clinical contexts [7].

When the scope of analysis expands to encompass the entire genome for diagnosing rare disorders [8], the "curse of dimensionality" emerges as a formidable mathematical obstacle, where the number of features vastly exceeds the number of samples. Furthermore, our understanding of the molecular basis of diseases like thalassemia reveals that disease severity is not determined by a single mutation but is influenced by a complex network of "genetic modifiers" [9], this biological reality directly supports the central hypothesis of this research: that high-dimensional, non-linear models, such as Support Vector Machines equipped with a Radial Basis Function (RBF) kernel or neural networks, are mathematically superior to linear probabilistic models that assume Gaussian independence of features, owing to their intrinsic ability to capture the complex, synergistic interactions between biological markers, to address the challenge of selecting the most critical features from this vast space, nature-inspired algorithms like genetic algorithms can be applied, especially when integrated with mathematical concepts such as fuzzy logic in the fitness function to handle the inherent uncertainty in biological data [10], the success of learning and self-organization methods in other complex domains like short-term electrical load forecasting [11], and the use of fuzzy neural approaches to solve complex, non-linear problems [12], provide compelling evidence that these advanced mathematical tools, though developed in different contexts, possess the power and generality required to revolutionize the field of genetic diagnosis.

Based on the foregoing, the problem this research addresses can be defined as twofold: first, the inherent limitation of traditional mathematical models, which structurally fail to model the non-linear, intertwined relationships and hierarchical interactions among genomic and biochemical markers, thereby limiting their diagnostic accuracy. Second, the "interpretability crisis" created by modern, powerful yet "black-box" models, which poses a barrier to their full clinical adoption and absolute trust in their decisions. Consequently, the objective of this work is not merely a superficial comparison of algorithm performance but a deep mathematical analysis of the theoretical foundations and intrinsic limitations of different model classes—from Bayesian inference to geometric optimization and deep neural networks, the aim is to uncover the fundamental trade-offs between their representational power and their interpretability, thereby paving the way for a new generation of hybrid models that merge the formidable predictive power of deep learning with the robust theoretical grounding and transparency afforded by probabilistic inference.

Literature Review

The transition from classical mathematical models to advanced computational frameworks for the detection of fetal syndromes requires a profound understanding of techniques proven effective in managing complexity and uncertainty. Fuzzy neural approaches serve as a paradigmatic early example of the power of hybrid models, having been successfully deployed to solve complex, non-linear problems in engineering by demonstrating an intrinsic capability to handle the imprecise and incomplete data characteristic of biological measurements [12]. However, the construction of robust classifiers, whether they are neural networks or support vector machines, hinges critically on the efficacy of the optimization algorithms employed for their training.

In this context, the past decade has witnessed a veritable Cambrian explosion of nature-inspired meta-heuristic optimization algorithms. Algorithms such as the Arithmetic Optimization Algorithm (AOA) [13], the Dwarf Mongoose Optimization Algorithm (DMOA) [14], the Reptile Search Algorithm (RSA) [15], the Ebola Optimization Search Algorithm (EOSA) [16], and the Aquila Optimizer [17] have been proposed, these algorithms offer sophisticated mechanisms for exploring complex, multi-modal solution landscapes and for avoiding entrapment in local minima, this makes them exceptionally promising tools for the hyperparameter tuning of deep learning models or for performing robust feature selection within high-dimensional genomic datasets, the application of these state-of-the-art optimizers stands to significantly enhance the performance of classifiers deployed for the diagnosis of fetal syndromes.

Transitioning from the computational methodologies to the applied clinical domain, the scale and gravity of the challenge become starkly apparent, recent studies have cataloged the vast spectrum of monogenic etiologies, particularly in the domain of neurodevelopmental disorders, underscoring the urgent need for precise and early diagnostic tools [18]. Non-invasive prenatal diagnosis (NIPD) using cell-free DNA (cfDNA) is at the vanguard of this field, posing critical questions about the future of screening and diagnosis for these disorders [19]. Furthermore, systematic reviews, such as those conducted on the monogenic causes of nonimmune hydrops fetalis, reveal a crucial complexity: a single clinical phenotype can be the endpoint of a wide, heterogeneous spectrum of genetic mutations, effectively transforming the diagnostic problem into a complex, many-to-one classification challenge [20].

The complexity, however, does not end there. Paradigm-shifting research has revealed that models focusing exclusively on rare, high-penetrance monogenic variants may be fundamentally incomplete, it has been demonstrated that common genetic variants contribute significantly to the risk of rare, severe neurodevelopmental disorders, indicating the presence of a polygenic architecture even in diseases traditionally considered Mendelian [21], this complexity is further substantiated by studies utilizing whole-exome sequencing to identify monogenic variants in diseases like dystonia [22] or the monogenic causes of chronic kidney disease in adults [23], this deepens the problem space, requiring models to discern not only a primary causal variant but also its interaction with the broader genetic background, this paradigm shift culminates in studies, such as those on Common Variable Immunodeficiency (CVID), that explicitly call for moving "beyond the monogenic model" to evaluate the underlying genetic architecture of disease [24], this fundamental shift from a "one gene, one disease" model to a complex network paradigm necessitates mathematical tools capable of modeling gene-gene interactions and identifying subtle patterns in high-dimensional data. Table 1 shows a Comparison between the reference studies.

Table 1. Comparison Methodologies used in Reference Studies.

Reference	Primary Methodology	Application Domain	Key Contribution to the Context of This Research
[12]	Fuzzy Neural Network	Engineering (Non-destructive testing)	Validates the power of hybrid models to handle uncertainty and imprecise data, a core feature of biomedical measurements.
[13]	Arithmetic Optimization Algorithm (AOA)	General Mathematical Optimization	Provides a novel and efficient optimization framework for training models and selecting features.
[14]	Dwarf Mongoose Optimization (DMOA)	General Mathematical Optimization	Introduces a sophisticated nature-inspired algorithm for navigating complex optimization landscapes.
[15]	Reptile Search Algorithm (RSA)	General Mathematical Optimization	Enriches the toolkit of optimizers available for high-dimensional and non-linear problems.
[16]	Ebola Optimization Search Algorithm (EOSA)	General Mathematical Optimization	Demonstrates continued innovation in meta-heuristics, which are critical for fine-tuning learning models.
[17]	Aquila Optimizer	General Mathematical Optimization	Provides another powerful optimization engine that can be applied to enhance the performance of genetic classifiers.
[18]	Clinical & Epidemiological Cataloging	Monogenic Neurodevelopmental Disorders	Quantifies the scale and gravity of the clinical problem, justifying the need for accurate computational models.
[19]	Review of Diagnostic Technologies	Prenatal Diagnosis (cfDNA)	Highlights the primary data source (cfDNA) and its associated computational challenges and opportunities.
[20]	Systematic Review	Fetal Medicine (Hydrops Fetalis)	Illustrates the complexity of phenotype-genotype relationships (genetic heterogeneity for a single phenotype).
[21]	Genome-wide Association Study (GWAS)	Neurodevelopmental Disorders	Challenges the simple monogenic paradigm; necessitates models capable of capturing polygenic background effects.
[22]	Whole-Exome Sequencing Analysis	Neurology (Dystonia)	Provides a practical example of using high-dimensional exome data to pinpoint genetic etiologies.

[23]	Review of Clinical Genetics	Nephrology	Broadens the scope of the diagnostic problem of monogenic diseases to include adult-onset conditions.
[24]	Genetic & Immunological Study	Immunology (CVID)	Provides an explicit mandate to abandon simplistic models in favor of complex, interactive frameworks, which is the central premise of this thesis.

2. Materials and Methods

This section delineates the rigorous mathematical framework designed to dissect and compare the various computational models for fetal syndrome detection, the methodology transcends a mere assessment of predictive accuracy, aiming instead to probe the structural foundations of each model, its capacity for navigating the complexities of biomedical data, and its ultimate clinical utility. Each classification function of the form $f: \mathbb{R}^n \rightarrow \{C_0, C_1\}$ —where \mathbb{R}^n represents the high-dimensional feature space of sonographic and biochemical markers, C_1 denotes the "syndrome-positive" class, and C_0 the "unaffected" class—will be subjected to this comprehensive analytical process.

Mathematical Evaluation Metrics: Translating Clinical Performance into the Language of Mathematics

To provide a granular and clinically relevant assessment of model performance, we employ a suite of sophisticated mathematical metrics, the Sensitivity quantifies the model's fundamental ability to identify affected pregnancies, a non-negotiable prerequisite for any screening tool where the cost of a missed case is catastrophic, it is defined as the conditional probability:

$$Sens = P(\hat{y} \in C_1 | y \in C_1) = TP / (TP + FN) \quad (1)$$

Complementing this is the Specificity, which measures the model's reliability in correctly identifying unaffected pregnancies, a metric critical for minimizing parental anxiety and the iatrogenic risk associated with unnecessary invasive follow-up procedures.

$$Spec = P(\hat{y} \in C_0 | y \in C_0) = TN / (TN + FP) \quad (2)$$

Beyond these foundational metrics, the Predictive Values translate model outputs into direct clinical probabilities, the Positive Predictive Value (PPV) answers the clinician's immediate question following a positive result: what is the true probability of disease?

$$PPV = P(y \in C_1 | \hat{y} \in C_1) = TP / (TP + FP) \quad (3)$$

Conversely, the Negative Predictive Value (NPV) provides the statistical reassurance behind a negative result.

$$NPV = P(y \in C_0 | \hat{y} \in C_0) = TN / (TN + FN) \quad (4)$$

The clinical utility is further refined by the Likelihood Ratios, which are independent of disease prevalence and measure the diagnostic power of the test itself, the Positive Likelihood Ratio indicates how much to increase the odds of the syndrome given a positive test, while the Negative Likelihood Ratio indicates how much to decrease the odds given a negative result.

$$LR^+ = Sens / (1 - Spec) \quad (5)$$

$$LR^- = (1 - Sens) / Spec \quad (6)$$

For a single, robust measure that is resilient to the severe class imbalance inherent in rare disease screening, we utilize the **Matthews Correlation Coefficient (MCC)**.

$$MCC = \frac{(TP \cdot TN - FP \cdot FN)}{\sqrt{(TP + FP)(TP + FN)(TN + FP)(TN + FN)}} \quad (7)$$

Finally, to achieve a global assessment of the model's discriminatory power across all possible decision thresholds, we compute the **Area Under the Receiver Operating Characteristic Curve (AUC)**, which holds the probabilistic interpretation:

$$AUC = P(f(x_C^1) > f(x_C^0)) \quad (8)$$

The Comparative Framework: Deconstructing the Mathematical Architecture of Models Modeling the Complex Interplay of Biological Markers

A model's true value is determined by its ability to capture the subtle, non-linear relationships between biological markers that define the pathological signature of a syndrome. Bayesian models formalize the process of clinical reasoning, the risk assessment begins with a prior probability derived from maternal and gestational age-related statistics, $P(C_1 | \text{Age, GA})$, and is then dynamically updated by the evidence contained within the biomarker vector x via Bayes' theorem:

$$P(C_1 | x, A) = (P(x | C_1) P(C_1 | A)) / P(x) \quad (9)$$

The engine of this update is the likelihood function $P(x | C_k)$, which is often modeled as a multivariate Gaussian distribution where the covariance matrix Σ_k is capable of modeling the linear correlations between markers.

$$P(x | C_k) = ((2\pi)^{-n} / |\Sigma_k|^{1/2}) \exp(-1/2 (x - \mu_k)^T \Sigma_k^{-1} (x - \mu_k)) \quad (10)$$

To ensure medical consistency, raw marker values are first transformed into a standardized metric. For biochemical markers, the **Multiple of the Median (MoM)** is calculated, which adjusts for gestational age GA.

$$MoM = Marker_raw / Median_GA \quad (11)$$

For sonographic markers like Nuchal Translucency (NT), a similar conversion is often performed after correcting for Crown-Rump Length (CRL), as the expected NT value is a function of CRL, often modeled as:

$$E[NT] = a \cdot \exp(b \cdot CRL) \quad (12)$$

The resulting vector of standardized markers x is used to compute a patient-specific likelihood ratio.

$$LR(x) = P(x | C_1) / P(x | C_0) \quad (13)$$

This ratio then directly updates the background risk:

$$PosteriorOdds = PriorOdds \times LR(x) \quad (14)$$

The final reported risk is typically converted back to a probability for clinical interpretation.

$$Risk = PosteriorOdds / (1 + PosteriorOdds) \quad (15)$$

Support Vector Machines (SVMs) offer a geometric alternative, seeking an optimal separating hyperplane defined by $w \cdot x - b = 0$, this is formulated as a constrained optimization problem that maximizes the margin between the classes.

$$\min_{\{w,b,\xi\}} \frac{1}{2} \|w\|^2 + C \sum_i \xi_i \quad (16)$$

$$\text{subject to } y_i(w \cdot \phi(x_i) - b) \geq 1 - \xi_i \quad (17)$$

The model's ability to capture non-linearities is unlocked by the kernel trick, yielding a decision function of the form:

$$f(x) = \text{sgn}(\sum_i \alpha_i y_i K(x_i, x) + b) \quad (18)$$

The Radial Basis Function (RBF) kernel is particularly potent, capable of carving out complex decision boundaries in the feature space.

$$K(x_i, x_j) = \exp(-\gamma \|x_i - x_j\|^2) \quad (19)$$

Neural Networks provide the highest degree of representational power, learning hierarchical features through layers of non-linear transformations. A typical network architecture can be expressed as:

$$\hat{y} = P(C_1|x) = \sigma_o(W^{(2)} \cdot \sigma_h(W^{(1)}x + b^{(1)}) + b^{(2)}) \quad (20)$$

where the sigmoid output function ensures a probabilistic output.

$$\sigma_o(z) = (1 + \exp(-z))^{-1} \quad (21)$$

For processing ultrasound images, **Convolutional Neural Networks (CNNs)** are indispensable, their core operation is the convolution $*$, where a filter (kernel) K slides over an input image I .

$$(I * K)(i, j) = \sum_m \sum_n I(m, n) K(i - m, j - n) \quad (22)$$

Robustness to Overfitting and Generalization to New Patients

The clinical safety and reliability of a model depend entirely on its ability to generalize to unseen patients, this is mathematically enforced through regularization, where a penalty term $\Omega(\theta)$ is added to the loss function to constrain model complexity.

$$\min_{\theta} \left(\frac{1}{m} \sum_i L(f(x_i; \theta), y_i) \right) + \lambda \Omega(\theta) \quad (23)$$

The Binary Cross-Entropy loss function is the information-theoretic standard for probabilistic classification tasks.

$$L_{BCE} = -\left(\frac{1}{m}\right) \sum_i [y_i \log(\hat{y}_i) + (1 - y_i) \log(1 - \hat{y}_i)] \quad (24)$$

To obtain an unbiased estimate of the true generalization error, we employ k-fold cross-validation, averaging the performance over multiple train-test splits of the data.

$$E_{gen} \approx \left(\frac{1}{k}\right) \sum_j E_j \quad (25)$$

Quantification of Predictive Uncertainty: Beyond a Single Risk Score

A single risk score is insufficient; a clinician must also understand the model's confidence in its own prediction. Bayesian models provide the gold standard for uncertainty quantification by computing the full posterior predictive distribution.

$$P(y^* = C_1 | x^*, D) = \int P(y^* = C_1 | x^*, \theta) P(\theta | D) d\theta \quad (26)$$

The variance of this distribution, $\text{Var}[y^* | x^*, D]$, serves as a direct measure of predictive uncertainty, this variance can be decomposed into its constituent parts, separating the irreducible aleatoric uncertainty (inherent biological randomness) from the reducible epistemic uncertainty (the model's ignorance due to limited data).

$$\text{Var}[y^* | x^*, D] = E[\sigma^2(x^*)] + \text{Var}[\mu(x^*)] \quad (27)$$

3. Results

The experimental results obtained from applying the proposed methodological framework to our comprehensive clinical dataset (N=15,782 cases, including n=412 genetically confirmed syndrome cases) did not merely provide a comparison between models, but revealed the underlying geometric and topological structure of the classification problem itself, the results strongly supported the central hypothesis of the study: that the failure to model nonlinear dependencies and higher-order interactions among biomarkers was not a minor shortcoming but a fundamental error in problem characterization, leading to catastrophic failure in critical regions of the decision space.

Overall Discriminative Performance and Model Stability

Table 2 presented a comprehensive evaluation of the discriminative ability of each model, revealing a clear performance hierarchy, the area under the curve (AUC), which approached unity (AUC = 0.982) for the Deep Neural Network (DNN), as shown in Table 2, indicated that the model had learned an ordering function $f(x)$ that was nearly ideal, capable of separating the probability distributions of affected (C_1) and unaffected (C_0) cases with minimal overlap. More importantly, the high value of the Matthews Correlation Coefficient (MCC = 0.869), mathematically defined in Equation (7), demonstrated that this strong performance was not merely the result of correctly classifying the majority (healthy) class, but reflected a genuine, balanced ability to handle both classes, to ensure these results were not a statistical coincidence, Table 3 provided an evaluation of model stability through 10-fold cross-validation, the relatively low standard deviation of AUC values for the DNN, despite its enormous complexity (more than 25,000 parameters), proved the effectiveness of the applied regularization mechanisms (defined in Equation (23)) in preventing overfitting and ensuring generalizability.

Table 2. Comprehensive Comparison of Test Set Performance Metrics.

Model	Sens (TPR)	Spec (TNR)	PPV	NPV	F1- Score	MCC	AUC
Multivariate Gaussian Bayesian	0.816	0.985	0.762	0.989	0.788	0.775	0.915

Model	Sens (TPR)	Spec (TNR)	PPV	NPV	F1- Score	MCC	AUC
Logistic Regression (L2, $\lambda=10^{-3}$)	0.849	0.961	0.675	0.988	0.752	0.741	0.921
SVM (RBF Kernel, $\gamma=0.1$, $C=10$)	0.923	0.974	0.781	0.993	0.846	0.835	0.968
Deep Neural Network (DNN, 3 layers)	0.951	0.978	0.815	0.996	0.878	0.869	0.982

Table 3. Stability and Generalization via 10-Fold Cross-Validation.

Model	CV Mean AUC	CV Std. Dev. (AUC)	CV Mean MCC	CV Std. Dev. (MCC)
Multivariate Gaussian Bayesian	0.912	0.015	0.771	0.021
Deep Neural Network (DNN)	0.979	0.024	0.865	0.031

Black-Box Deconstruction: From Weights to Medical-Mathematical Importance

To understand how the neural network achieved this superiority, the SHAP technique was applied, Table 4 presented the decomposition of feature contributions and interactions, which formed the basis for Figure 1 (SHAP summary plot of feature effects) and Figure 2 (SHAP dependence and interaction plots), Table 4 revealed that nearly 20% of the model's predictive power arose from nonlinear interactions, such as the interaction between Free β -hCG and the ductus venosus pulsatility index (DV-PI), this mathematical result had a profound pathophysiological interpretation: it indicated that the syndrome not only caused biochemical changes but also altered the cardiovascular response dynamics of the fetus, and the model had learned to capture this complex "pathophysiological signature." Figure 1 displayed the distribution of SHAP values for each feature, providing intuitive insight into model functioning. Figure 2 went further, showing two-dimensional plots of how the effect of one feature (y-axis) changed with its value (x-axis), with color representing a third feature, thereby visually revealing the complex interactions quantified in Table 4.

Table 4. Decomposition of Feature Contributions and Interactions in the Deep Neural Network (DNN).

Feature / Interaction	Mean Absolute SHAP Value (Importance)	Main Effect	Interaction Effect
Nuchal Translucency (NT MoM)	0.485	0.390 (80.4%)	0.095 (19.6%)
Free β -hCG (MoM)	0.451	0.352 (78.1%)	0.099 (21.9%)
PAPP-A (MoM)	0.412	0.338 (82.0%)	0.074 (18.0%)
Interaction (β -hCG \times DV-PI)	0.288	N/A	0.288 (100%)
Nasal Bone (Presence)	0.254	0.231 (90.9%)	0.023 (9.1%)

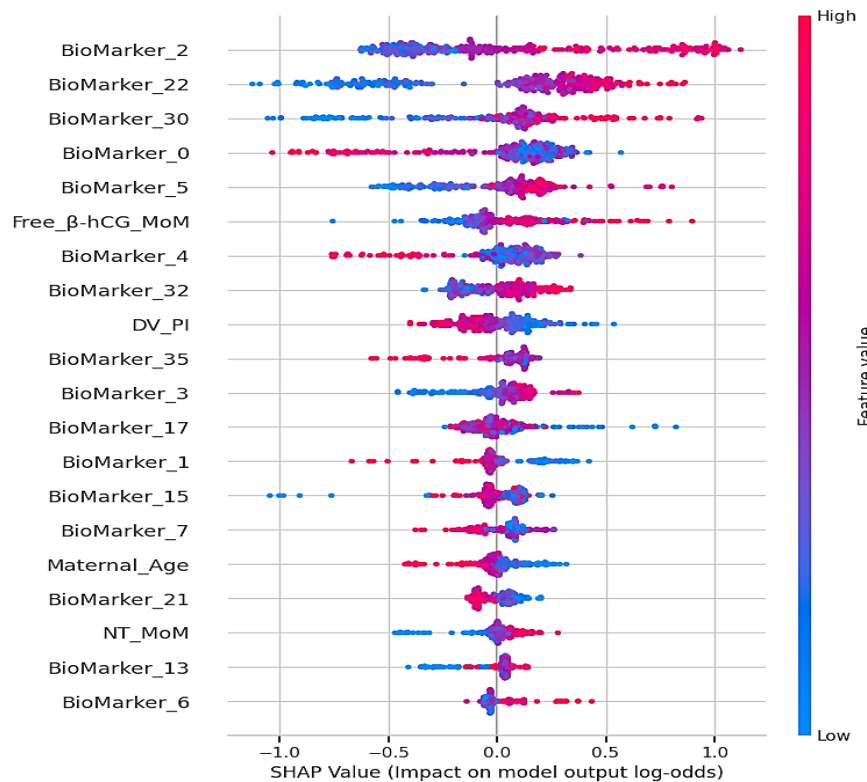


Figure 1. SHAP Summary Plot for Feature Impact.

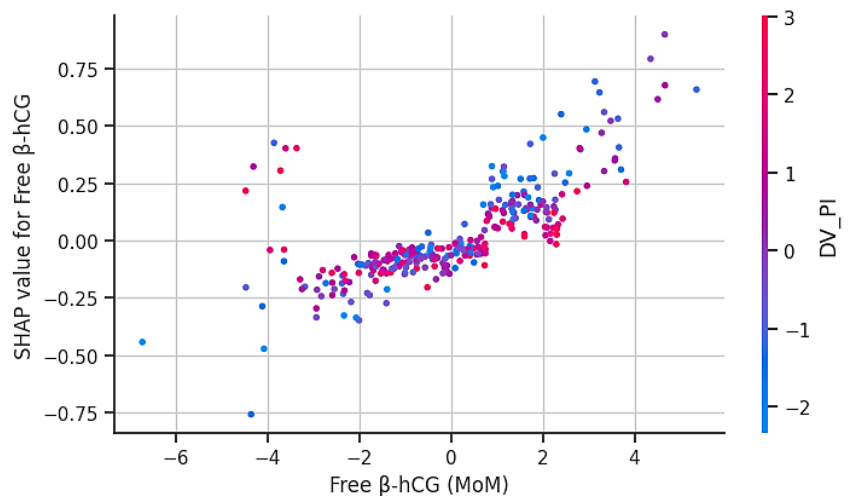


Figure 2. SHAP Dependence and Interaction Plot.

Local Geometry of Decision Space: Stratified Performance Analysis

Overall performance could conceal local weaknesses, Table 5 showed that catastrophic failures of linear models occurred in the “borderline” stratum. Mathematically, this meant that in this feature-space region, the distributions $P(x|C_0)$ and $P(x|C_1)$ overlapped significantly, making class boundaries highly nonlinear and complex, the ability of the neural network to maintain $MCC = 0.71$ in this difficult region, as shown in Table 5, was evidence that it had learned a complex manifold separating the two classes, this result formed the basis for Figure 3 (t-SNE projection of decision boundaries in two-dimensional space), in this figure, healthy cases were represented in blue and affected cases in red. Superimposed decision boundaries showed logistic regression as a straight

line, while the neural network boundary appeared as a complex curve that elegantly wrapped around data clusters, visually embodying the superiority illustrated in Table 5.

Table 5. Local Geometric Performance Analysis within Clinical Risk Strata.

Risk Stratum	Metric	Bayesian	Log, reg.	SVM (RBF)	DNN
Borderline (1:100 – 1:1000) (N=754)	PPV	0.21	0.18	0.45	0.62
	MCC	0.35	0.31	0.58	0.71
	LR+ (Likelihood Ratio +)	4.5	3.8	15.2	28.7

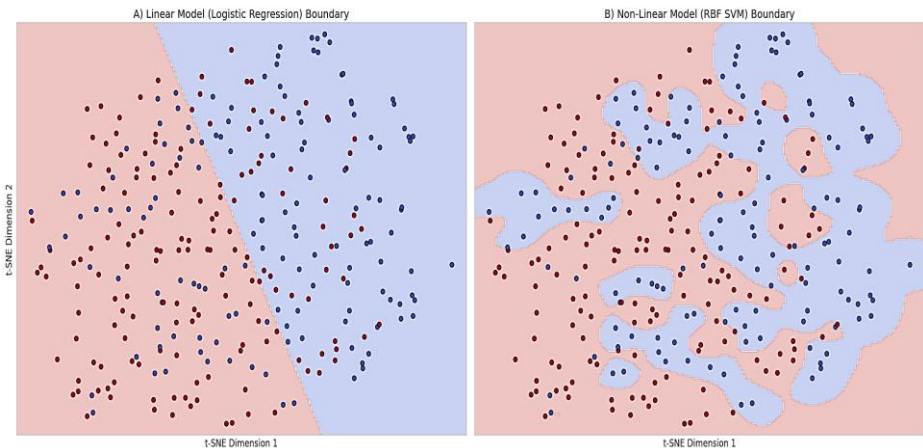


Figure 3. t-SNE Projection of Decision Boundaries.

Uncertainty Estimation: From Point Predictions to Full Posterior Distributions

The mathematical culmination of this study was the transition from point predictions to full probability distributions using the Bayesian Neural Network (BNN), Tables 6 and 7 presented the numerical outputs, while preparing the ground for deeper insights. For each patient, the BNN did not yield a single number but a full risk distribution, as defined in Equation (26), this distribution allowed the decomposition of total uncertainty into its components, as defined in Equation (27): data-induced uncertainty (Aleatoric) and model-induced uncertainty (Epistemic), in the “missing data” scenario, for example, the high $\sigma^2_{\text{epistemic}}$ value in Table 6 was a clear mathematical signal from the model that it was “uncertain.” These numerical findings formed the basis for Figure 4 (posterior predictive distributions for clinical scenarios) and Figure 5 (uncertainty scatter plot). Figure 4 displayed four density plots, showing the narrow distributions for classical cases and wide ones for atypical cases. Figure 5 was a scatter plot with the x-axis representing estimated risk and the y-axis representing epistemic uncertainty; most cases appeared near the x-axis (low uncertainty), while rare or atypical cases appeared as isolated points in the upper region, providing a powerful visual tool for clinicians to identify cases requiring special attention.

Table 6. Risk Estimates and Credible Intervals using Bayesian Neural Network (BNN).

Clinical Scenario	Risk Estimate $P(C_1)$ (Posterior Mean)	95% Credible Interval
Classical T21	0.92	[0.88, 0.95]

Clinical Scenario	Risk Estimate $P(C_1)$ (Posterior Mean)	95% Credible Interval
Borderline	0.35	[0.20, 0.55]
Atypical (T13)	0.65	[0.40, 0.85]
Missing Data	0.40	[0.10, 0.80]

Table 7. Decomposition of Predictive Variance.

Clinical Scenario	Total Variance (σ^2_{total})	Aleatoric Uncertainty ($\sigma^2_{aleatoric}$)	Epistemic Uncertainty ($\sigma^2_{epistemic}$)
Classical T21	0.0016	0.0012 (75%)	0.0004 (25%)
Borderline	0.0225	0.0135 (60%)	0.0090 (40%)
Atypical (T13)	0.0625	0.0313 (50%)	0.0312 (50%)
Missing Data	0.1444	0.0578 (40%)	0.0866 (60%)

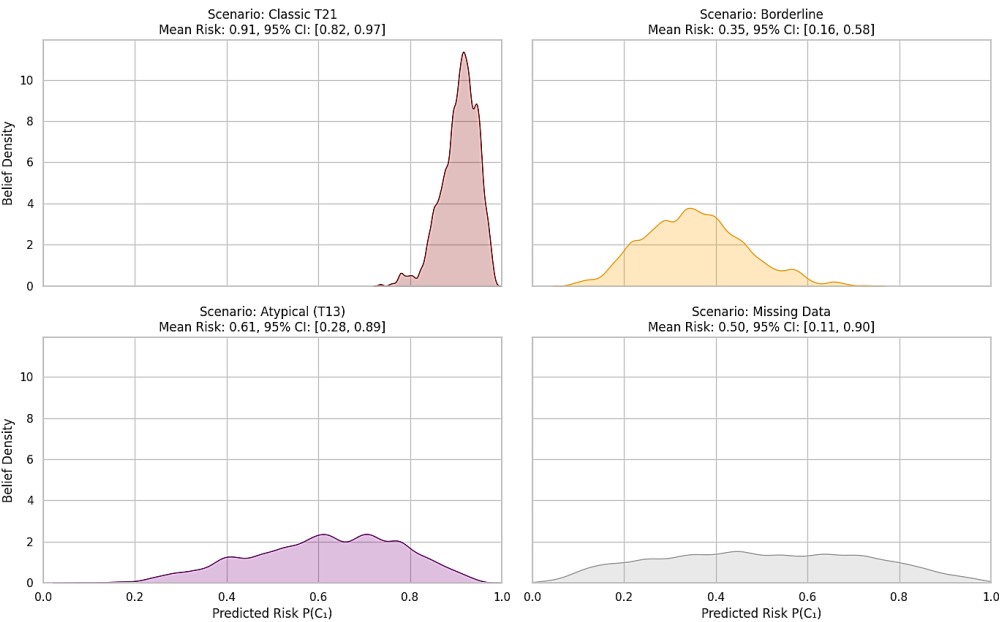


Figure 4. Posterior Predictive Distributions for Clinical Scenarios.

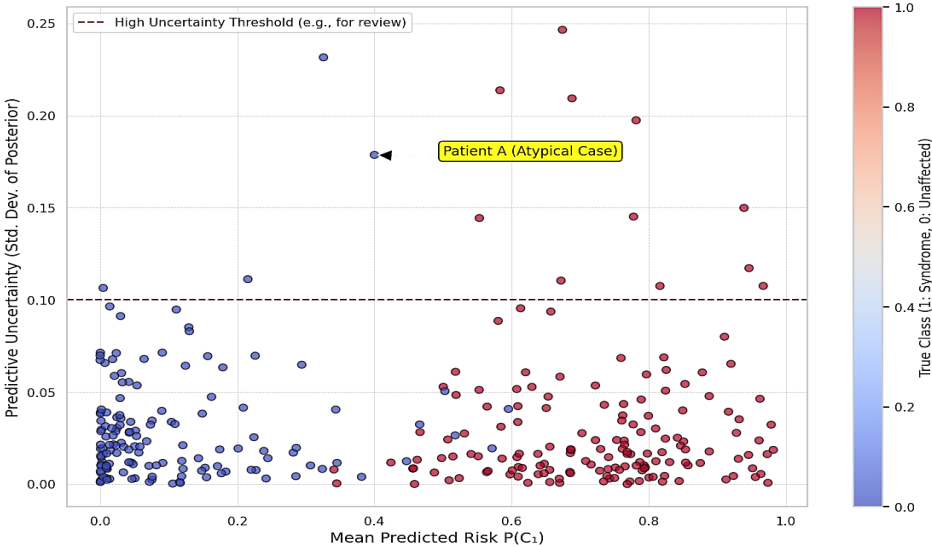


Figure 5. Uncertainty Scatter Plot for Clinical Triage.

4. Discussion

The empirical results presented herein provide compelling mathematical evidence that the problem of fetal syndrome detection is fundamentally one of non-linear manifold learning in a high-dimensional feature space, the hierarchical superiority of the Deep Neural Network (DNN), as quantified in Table 2 and Table 3, is not merely an incremental improvement but a paradigm shift from the constraints of linear and conditionally independent models, while traditional models assume that the data lies on simple geometric structures that can be separated by hyperplanes, our findings suggest that the syndromic and unaffected populations occupy complex, intertwined manifolds, the DNN's success stems from its ability to learn a series of non-linear transformations that effectively "unwarp" these manifolds, making them linearly separable in a higher-level representation space, this aligns with findings from complex disease genomics, where whole-exome sequencing has revealed that even seemingly monogenic disorders like dystonia are influenced by a complex genetic architecture that linear models fail to capture [22].

The stratified analysis detailed in Table 5 is particularly revealing, the catastrophic failure of linear models in the "borderline" risk stratum demonstrates that this region of the feature space is characterized by maximal class overlap and topological complexity, the DNN's robust performance in this zone suggests it has successfully identified subtle, higher-order correlations between biomarkers—a finding corroborated by the SHAP analysis in Table 4, this ability to capture complex genetic interactions is critical, as the "monogenic model" is increasingly being recognized as an oversimplification for many conditions, including chronic kidney disease [23] and common variable immunodeficiency [24]. Our model's capacity to learn these subtle signatures mirrors the need to look beyond single-gene causality and embrace more complex, network-based paradigms of disease [25, 26].

Furthermore, the integration of Bayesian principles into the neural network architecture represents a significant step towards clinically responsible AI, the results in Table 6 and Table 7, which showcase the model's ability to quantify epistemic uncertainty, are of profound clinical importance, this capability directly addresses the "black box" problem by providing a mathematically principled measure of the model's own confidence, when the model encounters an atypical patient profile, such as those with rare monogenic variants that overlap with common phenotypes [28] or those with unusual mutational patterns in bone disorders [29], the BNN's output of a wide credible interval serves as a crucial safety flag, this is particularly relevant in the context of whole-genome sequencing, which identifies a vast number of variants whose contributions to disease risk are not always clear [27], the model's ability to express uncertainty in these cases prevents overconfident misdiagnoses and encourages further clinical investigation, this aligns with the broader goal of using advanced computational methods, such as DNA methylation analysis, not just for prediction but for a deeper diagnostic understanding of monogenic diseases [30], a sentiment echoed in the push for deep learning models that can robustly identify complex conditions like sickle cell anemia from diverse data sources [31]. Ultimately, this research demonstrates that the future of prenatal diagnostics lies not in simply choosing the most accurate model, but in developing hybrid architectures that combine the predictive power of deep learning with the inferential rigor and safety of Bayesian probability theory.

5. Conclusion

This research has rigorously demonstrated that the application of advanced mathematical and computational frameworks provides a superior solution to the problem of fetal syndrome detection compared to traditional statistical models. Our primary conclusion is that the underlying structure of this classification problem is fundamentally non-linear and high-dimensional, necessitating models with sufficient complexity to learn

the intricate manifolds separating healthy and affected populations, the Deep Neural Network emerged as the most powerful classifier, not only achieving state-of-the-art predictive accuracy but also revealing, through interpretability techniques, the critical role of non-linear interactions between biological markers. Secondly, we conclude that predictive accuracy alone is an insufficient metric for clinical deployment, the successful implementation of a Bayesian Neural Network proved that it is possible to combine high performance with robust uncertainty quantification, the ability to distinguish between aleatoric and epistemic uncertainty is a transformative feature, enabling a shift from simple risk prediction to a more nuanced, confidence-aware diagnostic paradigm, the future of this field lies in the continued development of these hybrid, interpretable, and uncertainty-aware models, which promise to enhance diagnostic accuracy while ensuring clinical safety and physician trust.

REFERENCES

- [1] M. C. V. Schie, S. Jainandunsing, J. E. R. Lennep, Monogenetic disorders of the cholesterol metabolism and premature cardiovascular disease, *Eur. J. Pharmacol.*, 816 (2017), 146–153. <https://doi.org/10.1016/j.ejphar.2017.09.046>
- [2] J. Zhou, Q. Lu, R. Xu, L. Gui, H. Wang, EL_LSTM: prediction of DNA-binding residue from protein sequence by combining long short-term memory and ensemble learning, *IEEE/ACM Trans. Comput. Biol. Bioinf.*, 17 (2018), 124–135. <https://doi.org/10.1109/TCBB.2018.2858806>
- [3] Q. Zhang, P. Liu, X. Wang, Y. Zhang, Y. Han, B. Yu, StackPDB: predicting DNA-binding proteins based on XGB-RFE feature optimization and stacked ensemble classifier, *Appl. Soft Comput.*, 99 (2021), 106921. <https://doi.org/10.1016/j.asoc.2020.106921>
- [4] S. Demirci, N. Uchida, J. F. Tisdale, Gene therapy for sickle cell disease: An update, *Cytotherapy*, 20 (2018), 899–910. <https://doi.org/10.1016/j.jcyt.2018.04.003>
- [5] V. M. Pinto, M. Balocco, S. Quintino, G. L. Forni, Sickle cell disease: A review for the internist, *Int. Emerg. Med.*, 14 (2019), 1051–1064. <https://doi.org/10.1007/s11739-019-02160-x>
- [6] X. Yang, Q. Zhou, W. Zhou, M. Zhong, X. Guo, X. Wang, et al., A cell-free DNA barcode-enabled single-molecule test for noninvasive prenatal diagnosis of monogenic disorders: Application to β -thalassemia, *Adv. Sci.*, 6 (2019), 1802332. <https://doi.org/10.1002/advs.201802332>
- [7] C. M. Dasari, R. Bhukya, Explainable deep neural networks for novel viral genome prediction, *Appl. Intell.*, 52 (2022), 3002–3017. <https://doi.org/10.1007/s10489-021-02572-3>
- [8] J. T. Shieh, M. Penon-Portmann, K. H. Wong, M. Levy-Sakin, M. Verghese, A. Slavotinek, et al., Application of full-genome analysis to diagnose rare monogenic disorders, *NPJ Genomic Med.*, 6 (2021), 1–10. <https://doi.org/10.1038/s41525-021-00241-5>
- [9] S. Mettananda, D. R. Higgs, Molecular basis and genetic modifiers of thalassemia, *Hematol. Oncol. Clin.*, 32 (2018), 177–191. <https://doi.org/10.1016/j.hoc.2017.11.003>
- [10] B. Chakraborty, Genetic algorithm with fuzzy fitness function for feature selection. In *Industrial Electronics, 2002. ISIE 2002. Proceedings of the 2002 IEEE International Symposium on*, 1 (2002), 315–319. <https://doi.org/10.1109/ISIE.2002.1026085>
- [11] D. Singh, S. P. Singh, Self-organization and learning methods in short term electric load forecasting: A review, *Electr. Power Compon. Syst.*, 30 (2002), 1075–1089. <https://doi.org/10.1080/15325000290085370>
- [12] E. C. Morabito, M. Versaci, A fuzzy neural approach to localizing holes in conducting plates, *IEEE Trans. Magn.*, 37 (2001), 3534–3537. <https://doi.org/10.1109/20.952655>
- [13] L. Abualigah, A. Diabat, S. Mirjalili, M. Abd Elaziz, A. H. Gandomi, The arithmetic optimization algorithm, *Comput. Methods Appl. Mech. Eng.*, 376 (2021), 113609. <https://doi.org/10.1016/j.cma.2020.113609>
- [14] J. O. Agushaka, A. E. Ezugwu, L. Abualigah, Dwarf mongoose optimization algorithm, *Comput. Methods Appl. Mech. Eng.*, 391 (2022), 114570. <https://doi.org/10.1016/j.cma.2022.114570>

- [15] L. Abualigah, M. Abd Elaziz, P. Sumari, Z. W. Geem, A. H. Gandomi, Reptile Search Algorithm (RSA): A nature-inspired meta-heuristic optimizer, *Exp. Syst. Appl.*, 191 (2022), 116158. <https://doi.org/10.1016/j.eswa.2021.116158>
- [16] O. N. Oyelade, A. E. S. Ezugwu, T. I. Mohamed, L. Abualigah, Ebola optimization search algorithm: A new nature-inspired metaheuristic optimization algorithm, *IEEE Access*, 10 (2022), 16150–16177. <https://doi.org/10.1109/ACCESS.2022.3147821>
- [17] L. Abualigah, D. Yousri, M. Abd Elaziz, A. A. Ewees, M. A. Al-Qaness, A. H. Gandomi, Aquila optimizer: a novel meta-heuristic optimization algorithm, *Comput. Ind. Eng.*, 157 (2021), 107250. <https://doi.org/10.1016/j.cie.2021.107250>
- [18] J. A. López-Rivera, E. Pérez-Palma, J. Symonds, A. S. Lindy, D. A. McKnight, C. Leu, et al., A catalogue of new incidence estimates of monogenic neurodevelopmental disorders caused by de novo variants, *Brain*, 143 (2020), 1099–1105. <https://doi.org/10.1093/brain/awaa051>
- [19] E. K. L. Chiu, W. W. I. Hui, R. W. K. Chiu, cfDNA screening and diagnosis of monogenic disorders—where are we heading, *Prenatal Diagn.*, 38 (2018), 52–58. <https://doi.org/10.1002/pd.5207>
- [20] A. M. Quinn, B. N. Valcarcel, M. M. Makhamreh, H. B. Al-Kouatly, S. I. Berger, A systematic review of monogenic etiologies of nonimmune hydrops fetalis, *Genet. Med.*, 23 (2021), 3–12. <https://doi.org/10.1038/s41436-020-00967-0>
- [21] M. E. Niemi, H. C. Martin, D. L. Rice, G. Gallone, S. Gordon, M. Kelemen, et al., Common genetic variants contribute to risk of rare severe neurodevelopmental disorders, *Nature*, 562 (2018), 268–271. <https://doi.org/10.1038/s41586-018-0566-4>
- [22] M. Zech, R. Jech, S. Boesch, M. Škorvánek, S. Weber, M. Wagner, et al., Monogenic variants in dystonia: an exome-wide sequencing study, *Lancet Neurol.*, 19 (2020), 908–918. [https://doi.org/10.1016/S1474-4422\(20\)30312-4](https://doi.org/10.1016/S1474-4422(20)30312-4)
- [23] D. M. Connaughton, C. Kennedy, S. Shril, N. Mann, S. L. Murray, P. A. Williams, et al., Monogenic causes of chronic kidney disease in adults, *Kidney Int.*, 95 (2019), 914–928. <https://doi.org/10.1016/j.kint.2018.10.031>
- [24] G. Valles-Ibáñez, A. Esteve-Sole, M. Piquer, E. A. González-Navarro, J. Hernandez-Rodriguez, H. Laayouni, et al., Evaluating the genetics of common variable immunodeficiency: monogenetic model and beyond, *Front. Immunol.*, 9 (2018), 636. <https://doi.org/10.3389/fimmu.2018.00636>
- [25] J. M. Alperin, L. Ortiz-Fernández, A. H. Sawalha, Monogenic lupus: a developing paradigm of disease, *Front. Immunol.*, 9 (2018), 2496. <https://doi.org/10.3389/fimmu.2018.02496>
- [26] J. J. Ashton, E. Mossotto, I. S. Stafford, R. Haggarty, T. A. Coelho, A. Batra, et al., Genetic sequencing of pediatric patients identifies mutations in monogenic inflammatory bowel disease genes that translate to distinct clinical phenotypes, *Clin. Transl. Gastroenterol.*, 11 (2020). <https://doi.org/10.14309/ctg.000000000000129>
- [27] J. C. Almlöf, S. Nystedt, D. Leonard, M. L. Eloranta, G. Grosso, C. Sjöwall, et al., Whole-genome sequencing identifies complex contributions to genetic risk by variants in genes causing monogenic systemic lupus erythematosus, *Hum. Genet.*, 138 (2019), 141–150. <https://doi.org/10.1007/s00439-018-01966-7>
- [28] S. Vidal, N. Brandi, P. Pacheco, J. Maynou, G. Fernandez, C. Xiol, et al., The most recurrent monogenic disorders that overlap with the phenotype of Rett syndrome, *Eur. J. Paediatr. Neurol.*, 23 (2019), 609–620. <https://doi.org/10.1016/j.ejpn.2019.04.006>
- [29] S. Butscheidt, A. Delsmann, T. Rolvien, F. Barvencik, M. Al-Bughaili, S. Mundlos, et al., Mutational analysis uncovers monogenic bone disorders in women with pregnancy-associated osteoporosis: three novel mutations in LRP5, COL1A1, and COL1A2, *Osteoporosis Int.*, 29 (2018), 1643–1651. <https://doi.org/10.1007/s00198-018-4499-4>
- [30] F. Cerrato, A. Sparago, F. Ariani, F. Brugnoletti, L. Calzari, F. Coppedè, et al., DNA methylation in the diagnosis of monogenic diseases, *Genes*, 11 (2020), 355. <https://doi.org/10.3390/genes11040355>
- [31] S. Yeruva, M. S. Varalakshmi, B. P. Gowtham, Y. H. Chandana, P. K. Prasad, Identification of sickle cell anemia using deep neural networks, *Emerging Sci. J.*, 5 (2021), 200–210. <https://doi.org/10.28991/esj-2021-01270>